Cavity ring-down lossmeter using a pulsed light emitting diode source and photon counting

Jonathan E Thompson and Kyle Myers

Department of Chemistry, University of Nebraska at Kearney, Kearney, NE 68849, USA

E-mail: thompsonje@unk.edu

Abstract

A new mode of cavity ring-down measurements in which an incoherent, broadband light emitting diode (LED) is used as the spectroscopic source is described. Light from a pulsed LED (570 nm, 12 nm FWHM) was coupled into a 32 cm linear optical resonator and a ring-down waveform obtained on a gated photon counter. Cavity time constants observed were on the order of 3–4 μs, yielding effective optical path-lengths in excess of 1 km. In an effort to demonstrate the function of the instrument we have measured absorption and Rayleigh scattering by gases introduced into the measurement cell. Measurements of Rayleigh scatter by CO_2 and 1,1,1,2 tetrafluoroethane (R-134a) were used to calibrate the instrument. The Rayleigh extinction coefficients determined through the LED–CRD method were found to agree with literature values to within 12% on average. In an additional set of experiments, a laboratory-generated vapour containing either iodine or ozone was introduced into the measurement cell in an effort to demonstrate the technique's ability to monitor absorbing gases. The ring-down time constants (τ) observed were found to decrease by 15–75% when the absorbing gases were added to the measurement cell. The observed decrease in cavity time constant was proportional to the quantity of absorbing gas within the measurement cell. Minimum detectable extinction coefficients (2s) of $\approx 2.5 \times 10^{-7}$ cm^{-1} were achieved. The LED–CRD approach may lead to development of inexpensive gas sensors or monitoring systems for atmospheric extinction/visibility.

Keywords: cavity ring-down spectroscopy, gas-phase absorption, spectroscopic methods

(Some figures in this article are in colour only in the electronic version)

Introduction

Cavity ring-down spectroscopy (CRDS) is a highly sensitive approach to gas-phase absorption spectroscopy in which a stable optical resonator formed from two or more highly reflective mirrors is used to achieve path lengths on the order of 1–10 km within a relatively small (table-top) instrument package. In the CRDS experiment, a probe light beam is used to excite the optical resonator and then is rapidly switched off.

The probe beam continues to circulate between the mirrors of the resonator but this beam is attenuated slightly each round trip owing to absorption or scattering losses from the sample placed between the mirrors, and because the mirrors themselves are not perfect reflectors. On each pass, a small fraction of the circulating beam passes through each mirror and can be collected and measured as an indicator of intra-cavity light intensity. The light intensity (i) measured at such a detector is found to decay exponentially in time after the

pulse (t) according to

$$i(t) = i_0 \exp\left\{-[(1-R) + kL]\left(\frac{tc}{L}\right)\right\}, \qquad (1)$$

where R is the mirror reflectivity (typ. > 0.999), k is the sample extinction coefficient (per unit distance, often m^{-1}), L is the distance between the mirrors (m), and c is the speed of light ($m\,s^{-1}$). In a typical CRDS experiment, the time constant (τ) for this exponential decay is the variable which is measured experimentally. The time constant is the time required for $i(t) = i_0\,e^{-1} \approx 0.3679\,i_0$ and can be given by

$$\tau = \frac{t_r}{2[(1-R) + kL]}, \qquad (2)$$

where t_r is the time required for the light beam to make one round trip through the resonator (s), and the other variables are as previously described. If the time constant (τ) of an 'empty' resonator is found, the extinction coefficient (k) of the sample can be extracted from the data through

$$k = \frac{1}{c}\left(\frac{1}{\tau_{\text{sample}}} - \frac{1}{\tau_{\text{empty}}}\right). \qquad (3)$$

From these relationships, it can be seen that the value of τ is directly related to the rate of attenuation of the light beam within the resonator. For a measurement cell of fixed dimensions and mirror reflectivity, only changes in sample extinction coefficient (k) can give rise to measurable changes in ring-down time constant (τ). The CRDS technique can therefore be used to monitor the concentration of absorbers since extinction coefficient is linearly proportional to the concentration of the substance in question.

Traditionally, CRDS experiments have been conducted using either pulsed fixed frequency lasers [1, 2], or dye lasers [3–5]. These lasing systems provide the rapid on/off switching rise times (<100 ns) necessary to make CRDS measurements but are often bulky, expensive and consume considerable electrical power. These caveats limit the use of these lasers as components in inexpensive, portable optical sensing systems. A significant improvement in this regard has been the development of so-called continuous wave cavity ring-down measurements (cw-CRDS). In cw-CRDS, a narrow bandwidth continuous laser is used to excite the optical cell. After sufficient intra-cavity power builds, the laser is switched 'off' either by deflecting the beam with an acousto-optic modulator [6] or by creating a mismatch between laser frequency and allowed cavity modes such that light can no longer be coupled into the resonator [7, 8]. In either case, the ring-down transient is then recorded. The cw-CRDS approach has several documented practical advantages over the pulsed approach including improved spectral resolution, sensitivity and the possibility of using relatively inexpensive, compact cw diode lasers as sources [9–12]. However, the narrow bandwidth of the cw lasers employed most often necessitates that the cavity length is continuously modulated using a piezoelectric element so that the laser light can be periodically coupled into a cavity mode. Additionally, the high intra-cavity fluences that can be obtained can lead to saturation effects which may be undesirable in certain experiments. Also, while the frequency of these diode laser sources can often be altered slightly, the prospects for true broadband CRDS measurements (10–100 nm of spectral range) using these lasers seems limited.

In this account, we report the results of our investigation into the use of light emitting diodes (LED) as sources for cavity ring-down spectroscopy. To our knowledge, this is the first description of using LEDs as sources specifically for cavity ring-down measurements although Kebabian *et al* have previously explored their use for the related technique of cavity attenuated phase shift spectroscopy [13]. Using LEDs as sources for CRD offers several potential advantages over laser sources. LEDs are very inexpensive, consume negligible power compared to conventional laser sources, are available at a large number of optical frequencies, can be pulsed at high repetition rates, and typically emit light over a 10–50 nm range of wavelengths which could potentially allow for broadband measurements.

Unfortunately, light from LEDs is not well collimated and is difficult to couple into the ring-down cell efficiently. This leads to relatively low cavity output power available for measurement. Attempts to use traditional methods (oscilloscope with photomultiplier) to measure the ring-down decay transient have proven unsuccessful as the light intensity exiting the resonator is not sufficient to produce a consistent, standing current. Instead, a series of individual photon detection events (≈ 2 Mcounts s^{-1}) are observed. It was surmised a traditional ring-down transient could be obtained by counting photon arrival events in sequential time bins over many pulses of the LED and constructing a histogram of the number of counts in time.

In our approach to this experiment we have used the TTL trigger line of a standard function generator to pulse a yellow–green LED at 5–16.5 kHz. Light from the LED was coupled into a linear optical resonator and a photomultiplier tube was used to monitor the light exiting the optical cavity. Photon counting electronics were used to count photon arrival events in time over 30 000 pulses of the LED to obtain a traditional ring-down transient. To test this approach to CRD measurements we have added several gases to a measurement chamber which surrounds our optical cell. In one set of experiments, we have added varying amounts of ozone (O_3) and molecular iodine (I_2) to our test chamber. Both of these gases absorb light within our spectral bandwidth of detection [14, 15], and therefore would be expected to decrease the observed cavity time constant (τ). In a second set of experiments, we have added gases of known Rayleigh scattering losses in order to examine quantitative aspects of our measurement by comparing accepted Rayleigh scattering coefficients at room temperature and pressure with those obtained via measurement using our instrument and equation (3). In both sets of experiments, the ring-down time constant (τ) was observed to vary in an expected way when absorbers or scattering gases were present in the cell.

This report is meant to document the initial demonstration of the LED–CRD technique. Given the availability of LEDs and ring-down mirrors throughout the visible and near IR region of the spectrum, the measurement principle which is demonstrated could potentially be applied to create inexpensive sensors for a variety of gas phase species of atmospheric significance (including O_3, NO_2, NO_3, ClNO, halogens, etc...). Additionally, the technique may find use in measurements of visibility/atmospheric particulate matter. It is conceivable that LEDs could also be used for liquid phase ring-down measurements similar to those recently reported
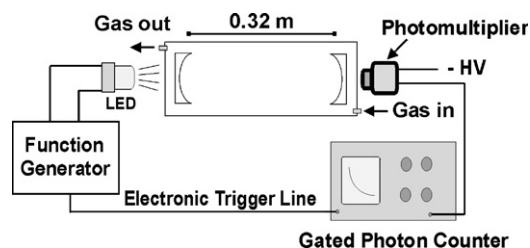
Figure 1. Illustration of the experimental setup for LED–CRD.

by several investigators [16–18]. Thus, it is believed the LED–CRD technique may be of general interest to many investigators in a variety of fields of study.

Experimental

Instrument

The experimental setup for our LED–CRD experiment is illustrated in figure 1. The cavity ring-down cell was constructed by separating two 2.03 cm diameter mirrors (6 m radius of curvature, $R = 0.9997$) by 0.32 m. The mirrors, which were in direct contact with the gases used, were enclosed in a Plexiglas box that served as the measurement chamber. One gas inflow and two gas outflow ports (one opening at the top and one at the bottom of the cell) were drilled at the ends of the box to allow for constant flow of gas through the cell. A pulsed LED source ($\lambda_{max} = 570$ nm, 12 nm FWHM, 7°) was driven by the TTL line of a function generator (Good Will Instrument Co. Ltd, Model GFG-8020G). The LED was operated with a drive current of 35 mA, which produced an estimated output power of ≈0.5 mW from the LED. The LED was placed at one end of the box, while a photomultiplier tube (Hammamatsu, Model 931B) was placed at the other end of the box. Both the LED source and the PMT were outside of the Plexiglas chamber, and a 2.54 cm diameter transparent section at each end of the box allowed for light to pass through. No focusing or beam steering optics were used to direct light into the measurement cell. The photomultiplier tube was biased at −1000 V by a high voltage power supply (Stanford Research Systems Inc., Model PS325/2500V-25W). The signal from the PMT was fed to a gated photon counter without pre-amplification (Stanford Research Systems, Multichannel Scaler Model 430). The internal 50 Ω load of the photon counter was used to convert the PMT current to a voltage for measurement. The gated photon counter and the function generator were connected with a trigger line in order to simultaneously trigger the pulsing of the LED source and data acquisition by the gated photon counter. Both the data acquisition trigger and discriminator trigger were set to the negative going pulse. The discriminator level that determined a 'count' for our experiments was −5 mV. All gas measurements used 3 000–15 000 individual 5 ns wide time bins, and the bin clock was controlled internally. Each ring-down decay transient was the sum of 30 000 individual records (pulses of the LED). An accurate determination of ring-down time constant requires the decay transient is adequately sampled. Thus, a bin width which is very narrow when compared with the value of τ is required. The 5 ns bin width used in our experiments provided ≈200–800 individual bins

(points) per time constant during our experiments which was adequate for curve fitting.

At first glance, it may seem the rate at which ring-down data can be collected would be determined by the frequency at which the LED is pulsed. However, this was not the case in our experiments. The number of individual ring-down experiments which could be performed each second was limited by the circuitry of the gated photon counter to be ≈250 under our operational parameters. Thus, it required approximately 120 s to obtain one ring-down transient produced from summing 30 000 individual LED pulses in our experiments.

Data analysis

Ring-down transients were collected and saved to disk. The time constants (τ) were extracted by deleting all data points that were outside of the ring-down curve, and by fitting a first-order exponential to the ring-down curve itself (Origin Software, Microcal Software, Inc.) The extinction coefficient for each gas sample was determined through equation (3). For this process, the 'empty' cavity ring-down time was that observed for helium gas. Helium was used as the empty cavity purge gas since it does not absorb in our measurement window and has an exceedingly small Rayleigh scattering cross section. Limit of detection was calculated as the extinction coefficient (k) which would cause a shift in the observed ring-down time equal to two standard deviations (s) from the blank (He) mean.

Gas calibration

Our instrument was calibrated by using helium, carbon dioxide and 1,1,1,2 tetrafluoroethane (a.k.a. Dupont SUVA or R-134a). The gases were allowed to flow from a pressurized gas tank to the cell through a 6 m tube which allowed for the gases to reach room temperature. A highly efficient filter (Mykrolis Wafergard) was fitted at the end of the 6 m tube to assure all particles are removed from the gas stream before entering the measurement chamber. A glass baffle (7.6 cm × 7.6 cm) was placed inside the cell at the gas inflow opening to stimulate mixing of gases in the cell. During experiments, one of the gas outflow openings (upper or lower) was plugged depending on the molecular weight of the sample gas in relation to air. This allowed maximum retention of the target gas within the sample chamber. The other gas outlet was kept open to prevent buildup of pressure in the chamber. The ring-down cavity cell was flushed for approximately 30 min with each gas before data was collected. Data reported represents the average of seven replicate trials with each trial being the mean of ten replicate measurements for each gas.

Iodine vapour experiment

An iodine vapour flow cell was constructed by splitting the air flow from a compressed air cylinder after travelling through the 6 m tube. One line went through a needle valve, which allowed for control of air flow entering this side of the split. This air flow then passed through a 3.1 cm diameter glass chamber fashioned from a weighing bottle that contained a few crystals of solid iodine at 20 °C. Iodine is known to sublime at room temperature and pressure (vapour pressure of

0.2–0.25 mm Hg) [19, 20] and we have used this property to create an I_2 vapour to measure with our LED–CRD technique. The other air flow from the split was simply diverted through a rubber tube. The two lines then recombined in a mixing tee and the combined flow entered the cavity cell. This splitting allowed for the dilution of iodine vapour prior to entering the cell, and the needle valve allowed for precise control of the amount of iodine flowing into the cell.

Using this apparatus we have attempted an experiment aimed at demonstrating monitoring of an absorber is possible with the LED–CRD technique. In this experiment, we sequentially increased the amount of iodine presented to our detection cell by slowly opening the needle valve described above. Initially, this valve was closed and ring-down times were collected when only filtered air was flowing through the cell. After 20 min, the needle valve was opened two full revolutions which allowed a small quantity of air to flow through the iodine chamber. After an additional 30 min, the valve was opened another full revolution and additional data was collected. Twenty-six minutes later, the valve was opened another full revolution allowing additional iodine to reach our measurement chamber. At this point, it was determined additional iodine vapour would completely suppress the ring-down signal and after 28 min the valve was completely closed, and ring-down times were collected as the filtered air flushed the iodine vapour from the measurement cell.

Ozone absorption experiment

Ozone was generated by flowing compressed oxygen through a commercial electrostatic discharge ozone generator (OREC Ozone Systems, V series) operated at 2.5 L min^{-1} gas flow rate. The stream from the ozone generator was then mixed with an air flow from a regulated compressed air tank inside of a stainless steel mixing tee. This air flow serves to dilute the ozone prior to measurement. The regulator outlet pressure for both the air and oxygen was approximately equal to 4–6 psi. Ozone concentrations within the measurement cell were then controlled by varying the current of the corona discharge. Initially, the ozone generator was turned off, and ring-down times were collected for the cell which contained the air/oxygen mix. After 22 min the ozone generator was turned to 30% of maximum ozone generating capacity, and ring-down transients were collected for this concentration of ozone. After 31 additional minutes the generator was then turned to 35% generating capacity, and ring-down decay waveforms were collected at this concentration for 18 more minutes. The ozone generator was then shut off, and ring-down curves were collected for 18 min as the air/O_2 mix flowed through the cell. It was observed that if the generator was set at a level any higher than 35% generating capacity, the concentration of ozone was too high for accurate ring-down measurements to be made.

Operation of the generator at 60% of maximum output is known to produce ozone at a rate of $\approx$0.5 mmol min^{-1}. Thus, after accounting for dilution with the air stream we are confident ozone concentrations in our measurement chamber were significantly less than $\approx$6 × 10^{16} cm^{-3} during our experiments. While providing an upper limit of the O_3 concentration is practical, estimating the standing ozone concentration within our measurement chamber based solely on the rate of O_3 generation and approximate gas flow rates is prone to significant error. The ozone which is produced in the generator undergoes a rapid decomposition so a significant fraction may decompose prior to measurement. Attempts to model this decomposition are confounded by the observations that the kinetics of ozone decomposition are highly dependent on conditions such as relative humidity, and the composition/previous use of the sample transfer line/storage chamber [21, 22].

Results and discussion

LED sources for CRD

An initial concern regarding the use of LEDs as a source for CRD measurements was the on/off switching time. Clearly, the rise time for switching should be much shorter than the ring-down time constant (τ). Other investigators have previously demonstrated sufficiently rapid switching of LEDs using custom drive circuits [23, 24]. For instance, O'Hagan *et al* [23] have designed and implemented a circuit that provides <5 ns pulses of LEDs. We have opted to use a laboratory function generator in our experiments for simplicity, and have found it to function adequately. To investigate the LED switching time we have directed light from the LED towards our photomultiplier which was interfaced to the gated photon counter. The optical resonator was not used in this experiment. It was found $\approx$35 ns was required for complete on/off switching of the LED. This agrees well with the rise time measured for the LED with a photodiode detector and oscilloscope, and the specified rise time for the TTL line of the function generator we have used.

The switching rise time achieved with our LED and function generator is clearly sufficient for use with the CRD measurements described in this report as the 35 ns switching time is 10–110 times shorter than the ring-down times we have observed. It should also be noted that we briefly investigated use of a type of white-light LED which incorporates a blue LED with phosphors to produce broadband visible emission. It was found this type of LED is not suitable for LED–CRD measurements because the phosphors exhibit radiative deactivation on a similar timescale as the CRD experiment and require $\approx$10 μs for complete on/off switching.

Proof of principle observations

Figure 2(a) illustrates a series of LED on/off cycles when a glass microscope slide was placed between the cavity mirrors and then removed from the ring-down cell. Figure 2(b) illustrates the figure blown up between 90–110 μs. On this scale, an exponential ring-down decay transient is clearly observed when the glass slide was removed from the cell (black trace), but not observed when the slide was present (grey trace). This phenomenon can easily be explained. A conventional UV-VIS spectrophotometer was used to measure the transmittance of the glass slide to be 0.905 near 570 nm. Therefore, the microscope slide imparted an optical loss of 9.5% each pass through the cell from reflection losses at the air/glass interface. Equation two predicts a per-pass loss of this magnitude would essentially eliminate the ring-down
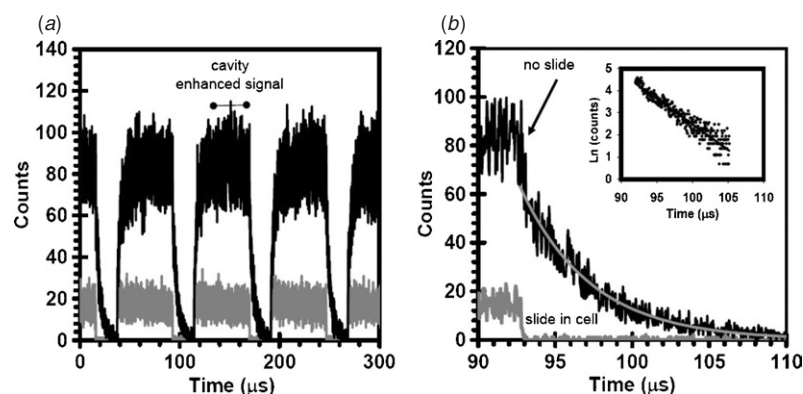
Figure 2. (*a*) Trace observed over several on/off cycles of the LED with (grey) and without (black) a glass microscope slide placed between the mirrors. The magnitude of the steady-state portion of the curve when the LED is 'on' represents the cavity-enhanced signal. To the left of this flat portion of each cycle waveform is the cavity 'ring-up' portion of the curve. To the right is the cavity 'ring-down' exponential we have used to extract data. (*b*) A close-up of the region between 90–100 μs. A ring-down transient is observed only when the glass slide is removed from the cell. Reflection losses from the microscope slide impart a 9.5% loss of intensity per pass which effectively eliminates the ring-down decay curve. Both A and B were collected using a photon counter bin width of 40 ns while ring-down waveforms used for quantitation were collected with a 5 ns bin width for improved sampling of the data.

transient altogether (predicted $\tau \approx 10$ ns) The observation that this occurs allows confirmation that the exponential decay observed was in fact due to the desired 'ring-down' effect and was not electronic in origin. Additionally, figure 2(*b*) demonstrates the resulting ring-down curve fits reasonably well to a first-order exponential (grey line and plot of Ln (counts) *versus* time being linear).

Another interesting aspect of figure 2(*a*) is that a 'ring-up' signal can be observed on the leading edge of each cycle as light intensity builds in the resonator. More importantly, the steady-state maximum (also referred to as '*cavity-enhanced*' signal) obtained when the LED was 'on' and after the cavity had fully 'rung-up' was observed to be four-fold higher in the trial in which the glass slide was absent from the measurement cell. The optical loss of 9.5% per pass has imparted a 75% reduction in steady-state signal. However, it should be noted that the experimental implementation of cavity-enhanced spectroscopy requires considerable effort be made to eliminate 'non-resonant' light (light not travelling between the mirrors) from reaching the detector when the LED is on. In practice, this often requires both spatial and spectral filtering. In our experiments, we have visually noted two sources of this 'non-resonant' light: (1) light scattered from the inside of the measurement chamber walls, and (2) emission from the LED outside of the stated wavelength range (red and blue emission observed). These observations were visible to the un-aided eye through the cavity output mirror. To generate the data presented in figure 2, the non-resonant light was eliminated through using a 580 $\pm$ 10 nm band-pass filter to effectively remove the undesired emission. Also, two partitions were placed within our cell and a hollow tube placed between the PMT and the output mirror to remove scattered, non-resonant light from reaching the detector. It should be noted that neither type of non-resonant light was found to alter the observed cavity time constant, but both forms had a large impact on the 'cavity-enhanced' steady-state signal observed when the LED was turned on. It is believed this results since both the scattered light and undesired emission occur only when the LED is energized. Nonetheless, the presence of non-resonant light

can cause significant systematic error when conducting cavity-enhanced spectroscopy experiments and must be eliminated to obtain accurate results.

Instrument calibration

The validation of quantitative results from ring-down experiments is often difficult due to a limited number of optical loss 'standards' available. Ideally, an investigator would like to fill the measurement chamber with an inert gas of known optical losses and test whether the CRD measurement yields this result for comparison. For absorbing gases, these attempts can be complicated by differences in detection bandwidth from experiment to experiment. Additionally, the high sensitivity and limited dynamic range of the ring-down approach requires per pass optical losses are rather small. For instance, a transmittance of 0.995 over our sample path (32 cm) would lead to a ring-down time of $\approx$200 ns which is essentially at the limit of our ability to obtain an accurate ring-down time constant. Therefore, even if detection bandwidth issues are not a problem, precise control over calibration gas concentration is required to assure the optical losses remain within the working range of the instrument.

An alternate and more user-friendly approach is to continuously purge the measurement cell with non-absorbing gases of known Rayleigh scattering loss. This approach is favourable for several reasons. Since Rayleigh scattering varies with probe frequency in a predictable way, one set of gases could potentially be used in many different spectral regions. Also, Rayleigh scattering is a spectrally broad phenomenon, which helps eliminate bandwidth effects. Additionally, given the low Rayleigh scattering cross sections of many gases, measurements near atmospheric pressure and room temperature are practical which eliminates the need for a vacuum cell and makes a flow-through sample cell feasible. Additionally, Naus and Ubachs [25] have previously used the CRD technique to verify Rayleigh scattering cross sections for several gases so literature precedent does exist for this type of measurement.
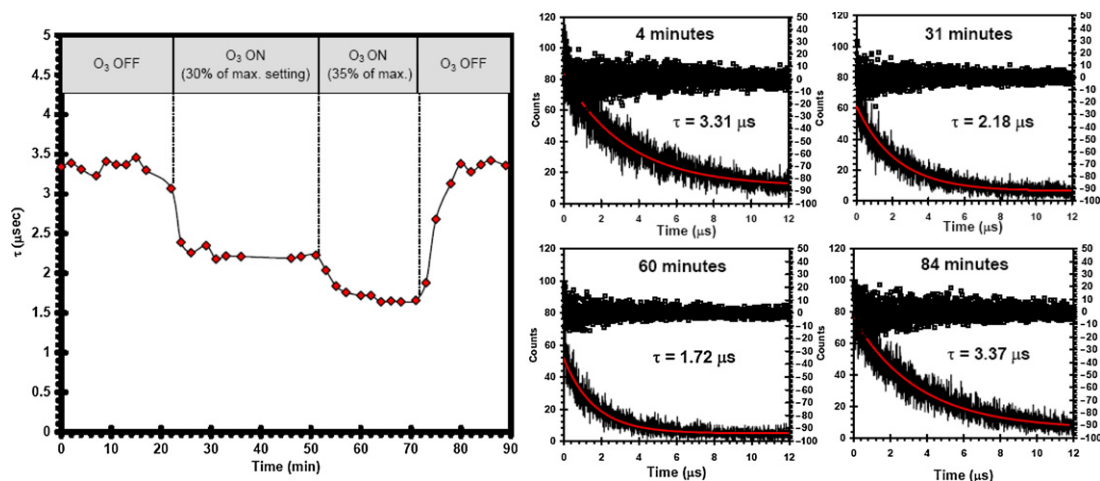
Figure 3. Left: illustration of how the observed ring-down time constant (τ) changed during an experiment in which ozone was generated and added to the measurement cell. The absorption maximum of the Chappius bands of ozone coincide with our measurement wavelength. This absorption gives rise to a clear decrease in cavity time constant as expected through equation (2). The cavity time constant was found to be inversely proportional to the rate of ozone production, and the time constant returned to 'normal' values within ≈8 min after switching off the ozone generator. Right: traces of actual ring-down decay curves, corresponding time constants (τ), and fit residuals for data points in each region of the plot shown on the left. The residuals are plotted on the second y-axis for clarity.

Table 1. Comparison of measured Rayleigh extinction coefficients (1 atm and 20 °C) with values from the literature. Data in parenthesis represent the standard deviation (s) of the measurement.

Gas	Measured value ($cm^{-1} \times 10^{-7}$ ($\pm 1\,s$))	Lit. value ($cm^{-1} \times 10^{-7}$)
CO_2	2.7 (± 1.0)	2.54[a]
R-134a (1,1,1,2 tetrafluoroethane)	8.5 (± 1.7)	7.20[b]

Data reported are the mean of seven independent analyses with each analysis consisting of ten replicate trials.
[a] Reference [28].
[b] Reference [29].

In an effort to examine our ability to extract accurate sample extinction coefficients (k) from our apparatus and equation (3), we have sequentially filled our measurement chamber with He, CO_2 and 1,1,1,2 tetrafluoroethane and measured resultant ring-down time constants for each sample. Helium was used as our 'empty cavity' purge gas since its Rayleigh scattering cross section is vanishingly small; some 200 times less than the value observed for CO_2 [26]. Our LED–CRD instrument is not nearly sensitive enough to detect a difference between the true evacuated (empty) cavity case and that in which He fills the sample chamber. As such, we have used the He purge ring-down times in place of the 'empty cavity' ring-down time for calculation of sample extinction coefficients through equation (3).

The results of this analysis are reported in table 1. For CO_2, we report a measured Rayleigh extinction coefficient of 2.7×10^{-7} cm^{-1} at 20 °C near atmospheric pressure which agrees with literature values to within 6%. The measured value for the extinction coefficient of R-134a by LED–CRD is ≈18% higher than the value reported in the literature. The cause of this discrepancy remains unclear; however, it should be noted the literature value is based on measurement of light scattered by the gas rather than measurement of attenuation of a beam passing through the gas. If a weak absorber is

present in the gas sample, it would have a very minor effect on the observed scattering signal, but could directly effect the attenuation measurement. Therefore, it is possible an absorbing contaminant is present in our SUVA calibration gas and this contaminant is leading to the observed difference in measurements. In any event, our LED–CRD measurement yields data of reasonable accuracy.

Laboratory monitoring experiments

In an effort to demonstrate monitoring of an absorbing gas is possible with LED–CRD we have added a laboratory generated ozone or iodine vapour to our measurement cell in separate experiments. The results of these experiments are shown in figures 3 and 4. These experiments are meant to demonstrate proof of concept—that monitoring absorbing gases is possible with the LED–CRD technique. As such, the method has not been optimized to eliminate interferences which may be encountered in 'real-world' applications and further development would likely be necessary to apply LED–CRD to a specific monitoring application.

Figure 3 illustrates the ozone monitoring experiment. Our measurement wavelength (570 nm) is near the absorption maximum of the Chappuis bands of ozone. This visible absorption feature is much weaker than the UV Hartley and Huggins bands which are typically used for absorption-based ozone measurements. Nonetheless, the ozone generation system we employed produced more than adequate quantities of ozone to easily observe a variation in ring-down time constant. Initially, the ozone generator was turned off and ring-down traces recorded for a sample that contained an air/oxygen mixture. As observed in the figure, ring-down times were initially slightly under 3.5 μs. The generator was then turned on to 30% of maximum ozone output while continuing to record ring-down transients. As the ozone flowed into the measurement cell, we observed an immediate decrease in ring-down time constant to the 2.2 μs range

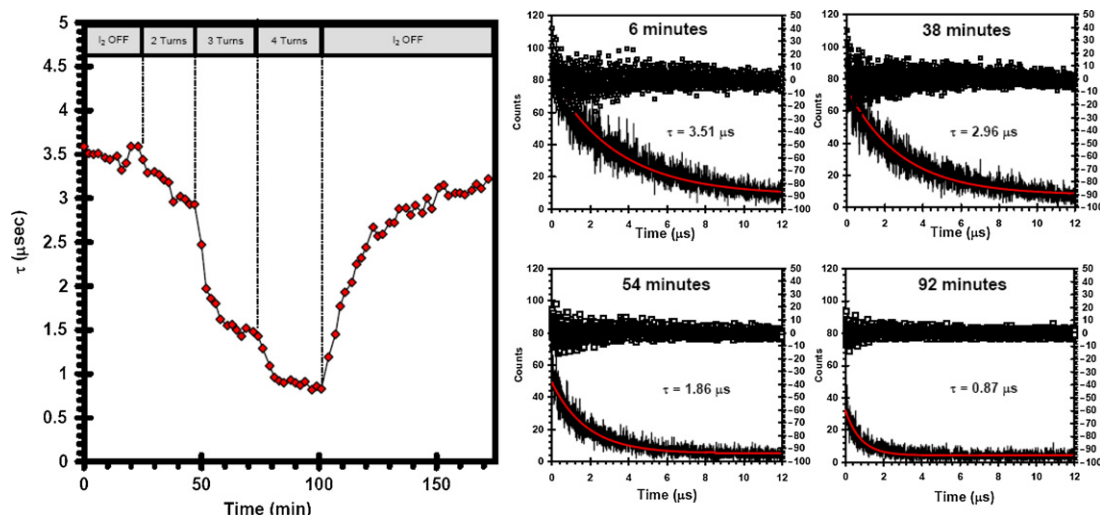**Figure 4.** Left: illustration of the effect of varying amounts of iodine (I_2) vapour on observed ring-down time constant (τ). A needle valve controlling the flow rate of iodine into the measurement cell was opened to various degrees at different times during this experiment (2 turns, 3, 4, closed). Upon opening the valve, the cavity time constant decreased indicating more absorbing I_2 is present. Upon closing the valve, the cavity time constant was observed to return to baseline in 60–70 min. Right: traces of actual ring-down decay curves, corresponding time constants (τ), and fit residuals for data points in each region of the plot on the left. The residuals are plotted on the second *y*-axis for clarity.

which would be expected after introduction of an absorber into the measurement cell. The generator output was then quickly ramped up to 35% of maximum capacity and again we observed an immediate decrease in ring-down time constant. Finally, the O_3 generator was switched off and within 8 min the values of τ observed returned to the 3.5 μs range.

The work of Burkholder and Talukdar [15] allows us to estimate the average absorption cross section of O_3 to be $\sigma = 4.5 \times 10^{-21}$ cm^2 over the bandwidth of our instrument. Estimation of the extinction coefficient of the sample placed in the chamber through equation (3) yields values in the 5.0×10^{-6}–1.0×10^{-5} cm^{-1} range for 30% and 35% ozone generating capacity, respectively. Given the previous estimate of absorption cross section, this corresponds to ozone concentrations within our cell in the 40–90 ppmv range.

Figure 4 illustrates a similar experiment in which an iodine vapour was generated with the flow cell described previously and directed into the measurement cell. Initially the needle valve controlling flow through the iodine chamber was closed and ring-down transients recorded with an air-filled measurement chamber. The needle valve was then opened two turns which allowed a very small amount of iodine vapour to flow into the measurement cell. After a few minutes, the valve was then opened a third and fourth full turn allowing additional iodine to reach the measurement cell. Finally, the needle valve closed and filtered air began flushing out the sample chamber.

As illustrated in figure 4, the cavity ring-down time constant was observed to decrease almost immediately after opening the valve, and increase when the valve was closed and the iodine flushed from the measurement chamber. In many regards the results of this experiment are very similar to those obtained for the ozone experiment described earlier— the cavity time constant varied in an expected way when an absorbing gas was added to the measurement chamber. More specifically, extinction coefficients between 1.5×10^{-6}–3.0×10^{-5} cm^{-1} were observed for the varying concentrations of iodine. One noticeable difference between

the iodine and ozone experiment is the time necessary for the ring-down time constant to return to values observed at the beginning of the experiment. For the ozone experiments, the time constant returned to 'normal' values within 8 min. During the iodine experiments, the time required was much longer, >60 min. This observed difference is likely due to a combination of rapid ozone decomposition and slow de-sorption kinetics of iodine which may have adsorbed on our measurement chamber walls during the experiment. In any event, figures 3 and 4 demonstrate the feasibility of the LED–CRD approach for measurement of gas-phase absorbers. Additional measurements aimed at correlating our CRD measurement with other independent measures of ozone or iodine concentration would be attractive to provide further validation of our approach.

Multi-exponential decay

As with any absorption spectroscopy, the spectral bandwidth of detection in LED–CRDS is of considerable importance. Zalicki and Zare [27] have considered bandwidth effects in CRDS and have found that the exponential decay model is valid only when the linewidth of the absorption feature is much broader than the bandwidth of the light circulating in the cavity. A similar, more general argument could be made for a case in which the absorption cross section of a species of interest varies significantly over the bandwidth of detection. If the spectral bandwidth of detection is not sufficiently narrow, ring-down waveforms which exhibit multi-exponential decay can result as wavelengths corresponding to the molecular resonance decay more rapidly than off-resonance light. This is clearly a concern should broadband LED–CRD be applied to measurements of gases with fine absorption features.

However, in our measurements of Rayleigh scatter and absorption by ozone and molecular iodine, we have not observed multi-exponential decay waveforms. This is evidenced by the right side of figures 3 and 4 which illustrate

the ring-down waveform observed, first-order exponential fit, and resulting fit residuals for both the ozone and iodine experiments. In all cases, plots of the observed residual in time seem to be symmetrically distributed around 0, which would be expected for a single exponential decay. Despite not being observed in our experiments, multi-exponential decay waveforms are certainly possible and should be considered in any future application of the LED–CRD technique.

Conclusions and future directions

A new mode of cavity ring-down measurements using a pulsed LED and photon counting has been demonstrated. This approach has been shown to yield quantitative results of reasonable accuracy, and detection limits comparable to other pulsed ring-down experiments. The technical advantages of this approach are tied to the use of the LED as a source. LEDs are very inexpensive, can be pulsed at a high frequency with simple drive electronics, are available at a number of wavelengths, and emit radiation over a range of wavelengths. The broad emission spectrum of the LEDs may allow for wavelength scanning in future versions of the LED–CRDS experiment. At present, the technique is limited by the low intensity of the output signal. In contrast to more conventional ring-down measurements, it is not possible to obtain a ring-down trace from each pulse of the incident light, but rather the summation of many individual pulses must be used. Filtering of the LED to improve spectral resolution will decrease the cavity output power substantially making obtaining a ring-down transient even more challenging. Thus, it may prove very difficult to match the high spectral resolution obtained with traditional laser source CRDS measurements. As such, the LED–CRD technique is unlikely to find use for very high-resolution measurements, but is certainly suitable, and perhaps preferable for monitoring applications in which very high spectral resolution is not needed.

If the efficiency with which light from the LED is coupled into the resonator and/or the brightness of the LED source can be improved significantly, replacement of the photon counter by an oscilloscope may be possible in future LED–CRD instruments. This may prove to be an important development as it would further reduce the cost/complexity of the instrument and allow for kHz ring-down curve collection rates. Another alternative would be to further explore cavity-enhanced spectroscopy with the LED source. As this technique measures the steady-state cavity output power, there would be no need to pulse the LED nor use sophisticated detection electronics to extract the resultant ring-down decay transient. However, to obtain accurate results extreme care must be taken to remove non-resonant light from the system, and the cavity-enhanced method would be subject to complications due to both source or detector drift.

References

[1] Thompson J E, Smith B W and Winefordner J D 2002 *Anal. Chem.* **74** 1962–7
[2] Sappey A D, Hill E S, Settersten T and Linne M A 1998 *Opt. Lett.* **23** 954–5
[3] Yu T and Lin C 1993 *J. Am. Chem. Soc.* **115** 4371–2
[4] Labazan I, Rudic S and Milosevic S 2000 *Chem. Phys. Lett.* **320** 613–22
[5] Ramponi A J, Milanovich F P, Kan T and Deacon D 1988 *Appl. Opt.* **27** 4606–8
[6] Romanini D, Kachanov A A, Sadeghi N and Stoeckel F 1997 *Chem. Phys. Lett.* **264** 316–22
[7] He Y and Orr B J 2000 *Chem. Phys. Lett.* **319** 131–7
[8] Schultz K J and Simpson W R 1998 *Chem. Phys. Lett.* **297** 523
[9] Bucher C R, Lehmann K K, Plusquellic D F and Fraser G T 2000 *Appl. Opt.* **39** 3154–64
[10] Romanini D, Dupre P and Jost R 1999 *Vib. Spectrosc.* **19** 93–106
[11] Crosson E R *et al* 2002 *Anal. Chem.* **74** 2003–7
[12] Mazurenka M I, Fawcett B L, Elks J M F, Shallcross D E and Orr-Ewing A J 2003 *Chem. Phys. Lett.* **367** 1–9
[13] Kebabian P L, Herndon S C and Freedman A 2005 *Anal. Chem.* **77** 724–8
[14] Calvert J G and Pitts J N Jr 1966 *Photochemistry* (New York: Wiley)
[15] Burkholder J B and Talukdar R K 1994 *Geophys. Res. Lett.* **21** 581–4
[16] Snyder K L and Zare R N 2003 *Anal. Chem.* **75** 3086–91
[17] Bahney B, van der Sneppen L, Wiskerke A E, Ariese F, Gooijer C and Ubachs W 2005 *Anal. Chem.* **77** 1188–91
[18] Hallock A J, Berman E S F and Zare R N 2002 *Anal. Chem.* **74** 1741–3
[19] Gillespie L J and Fraser L H D 1936 *J. Am. Chem. Soc.* **58** 2260–3
[20] Baxter G P, Hickey C H and Holmes W C 1907 *J. Am. Chem. Soc.* **29** 127–36
[21] Zaslowsky J A, Urbach H B, Leighton F, Wnuk R J and Wojtowicz J A 1960 *J. Am. Chem. Soc.* **82** 2682–6
[22] Mueller F X, Loeb L and Mapes W H 1973 *Environ. Sci. Technol.* **7** 342–6
[23] O'Hagan W J, McKenna M, Sherrington D C, Rolinski O J and Birch D J S 2002 *Meas. Sci. Technol.* **13** 84–91
[24] Araki T and Misawa H 1995 *Rev. Sci. Instrum.* **66** 5469–72
[25] Naus H and Ubachs W 2000 *Opt. Lett.* **25** 347–9
[26] Shardanand and Prasad Rao A D 1977 Absolute Rayleigh scattering cross sections of gases and freons of stratospheric interest in the visible and ultraviolet regions *NASA Technical Note* D-8442
[27] Zalicki P and Zare R N 1995 *J. Chem. Phys.* **102** 2708–17
[28] Cutten D R 1974 *Appl. Opt.* **13** 468–9
[29] *Reevaluation of HFC 134a (SUVA) Span Gas Multiplier* Air Resource Specialists Inc., Fort Collins, CO, July 2005